

On the Structure-Activity Relationship for NO-SCR with NH₃ Catalyzed by Cu-exchanged Natural Chabazite and SSZ-13

Julio C. López-Curiel, Gabriela I. Hernández-Salgado, María E. Hernández-Terán, Gustavo A. Fuentes*

Departamento de Ingeniería de Procesos e Hidráulica, Universidad A. Metropolitana - Iztapalapa, CDMX 09345, México.

*Corresponding author: Gustavo A. Fuentes, email gfuentes@xanum.uam.mx

Received July 16th, 2020; Accepted November 20th, 2020.

DOI: <http://dx.doi.org/10.29356/jmcs.v65i1.1267>

Abstract. In spite of their similar structures, the catalytic properties of natural and synthetic (SSZ-13) Chabazite during the selective reduction of NO with NH₃ have a different dependence on the Cu exchange level when tested under conditions equivalent to those found in Diesel vehicles. At low (1-2 wt.%) and high copper loadings (6-14 wt.%), their activities differ, because there are variations in the different species of Cu (Cu⁺, Cu²⁺, Cu-O-Cu) detected by UV-Vis. At intermediate Cu loadings (2-3 wt.%) they have similar high activities, reaching 100 % conversion. High deNO_x activity per Cu site appears to correlate with the predominance of charge compensation Cu²⁺ species over CuOx moieties. There are changes in the distribution of Cu moieties during operation of both catalysts, evidenced by DR-UV-Vis.

Keywords: Selective catalytic reduction of NO; Cu-CHA; natural chabazite; SSZ-13; UV-Vis.

Resumen. A pesar de sus estructuras similares, las propiedades catalíticas de Chabazita natural y sintética (SSZ-13) durante la reducción selectiva de NO con NH₃ dependen de manera diferente frente al nivel de intercambio con Cu cuando se prueban bajo condiciones equivalentes a las de vehículos Diesel. A bajos (1-2 % p/p) y altos contenidos de Cu (6-14 % p/p) la reducción de NO es diferente debido a variaciones en las distintas especies de Cu (Cu⁺, Cu²⁺, Cu-O-Cu) observadas por UV-Vis. Por su parte, los catalizadores intercambiados con 2-3 % p/p de Cu tuvieron alta actividad por sitio de Cu, alcanzando 100 % de conversión de NO, lo que parece deberse a la predominancia de especies de Cu²⁺ sobre especies CuOx de acuerdo con el análisis por DR-UV-Vis, el que también muestra la existencia de variaciones en la distribución de especies de Cu debido a la reacción.

Palabras clave: Reducción catalítica selectiva de NO; Cu-CHA; chabazita natural; SSZ-13; UV-Vis.

Introduction

Diesel engines are important because of their fuel efficiency and high power. They compare favorably with gasoline engines in terms of their raw NO_x emissions, but they do so under highly oxidative conditions, where the well-established 3-way converters are not operational. The main technology capable of operating under such conditions is the selective catalytic reduction of NO, particularly with ammonia (NH₃-SCR-NO). The preferred catalysts are Cu-Zeolite or Fe-Zeolite [1–4]. The zeolites with a Chabazite structure (CHA) have shown high activity and selectivity to N₂ in a wide temperature range, in addition to having high hydrothermal

stability, caused by the small size of their pores [5,6]. The recent technological trends involve the use of catalysts containing synthetic Cu-chabazite with different Si/Al ratios and metallic loads (SSZ-13, SSZ-39, and SAPO-34) [5,7–11], and that has left natural chabazite aside, in spite of its possible use in retrofitting emission control systems. There are practically no studies aimed at clarifying the differences between natural and synthetic zeolites and their application in SCR-NO with NH₃.

In this work, we compare the activity and selectivity during NH₃-SCR-NO of natural chabazite (CHA) and synthetic chabazite (SSZ-13) by varying the metallic loading of Cu. We tested the performance of the resulting catalysts at high space velocities (SV) and studied the distribution of Cu species using UV-Vis diffuse reflectance spectroscopy.

Experimental

Catalyst synthesis

The natural zeolite used in this study was provided by St. Cloud Zeolite from their Bowie (Arizona) natural chabazite deposit and is denoted as CHA_{raw}. The composition of CHA_{raw} is: 68.1 wt.% SiO₂, 18.59 wt.% Al₂O₃, 0.27 wt.% CaO, 0.75 wt.% MgO, 8.32 wt.% Na₂O, 1.12 wt.% K₂O and 2.84 wt.% Fe₂O₃. It has a Si/Al ratio of 3.5. In the following, this sample will be denoted as CHA_{nat}. The SSZ-13 was synthesized using a procedure similar to that described by Zones and the Lobo group to obtain a material with a Si/Al ratio of 12. [5,6,12]

Cu-CHA_{nat} was prepared using two-step solution ion exchange. First, CHA_{nat} was exchanged to Na-CHA_{nat} in 1 L of a 0.1 N NaNO₃ solution at room temperature for 12 h. It was then washed with deionized water and dried at 120 °C to obtain the Na-CHA_{nat} powder. A second ion exchange to produce the Cu-form of the zeolites was carried out at room temperature for 12 h in aqueous solutions containing different concentrations of Cu ((CH₃COO)₂.H₂O; 5.6x10⁻⁴, 2.25x10⁻³, and 9x10⁻³ M) in order to obtain final Cu loadings in the 1.3–6.5 wt.% range. After ion exchange the samples were filtered, washed with 250 mL of deionized water, dried at 110 °C for 3h and calcined in static air at 600°C for 3h.

In the case of Cu-SSZ-13, the Cu-form was prepared starting from H-SSZ-13 and Cu (CH₃COO)₂ H₂O aqueous solutions with different concentrations (2.25x10⁻³, 0.05, and 0.1 M). Ion exchange was carried out at room temperature for 12 h at a pH of ~3.5. After the exchange, the samples were filtered, washed with deionized water, and calcined in static air at 600 °C for 3 h. The final Cu loading ranged between 1.2 and 14.8 wt.%. All catalysts were stored at room temperature in a desiccator afterwards. The samples were named xx/CHA_{nat} or xx/SSZ-13, where xx indicates the Cu % content.

Catalyst characterization

Atomic Absorption Spectroscopy (SpectAA 20 FS, Varian) was used to determine Si, Al, Cu and Fe content in the natural chabazite, SSZ-13 and catalysts. The Si/Al ratio was determined to be ~ 3.5 for CHA catalysts. In the literature, it is mentioned that the Si/Al ratio of the natural chabazite is 3.1 [13], but we explain the difference as caused by the variability in the composition of the mined material. SSZ-13 catalysts had a Si/Al ratio of 12. The natural zeolite had a significant amount of Iron (Fe) which remained constant after exchange; table 1 shows the elemental composition of the calcined catalysts.

The crystalline structure of the zeolites was obtained from powder X-ray diffraction (XRD) using a Bruker AXS D8 diffractometer with Cu K α radiation. ($\lambda=1.542 \text{ \AA}$). The tube voltage was 40 kV and the current was 20 mA. The XRD patterns were collected in the 4 to 50° 2 θ range at a scan speed of 4 degrees min⁻¹.

The specific surface area and pore volume of the catalysts were obtained from N₂ adsorption-desorption analysis at 77.2 K (Autosorb-1, Quantachrome). Before the N₂ physisorption, each sample was degassed at 300°C for 12 h under vacuum to remove adsorbed water. The surface area and mesopore volume were determined by using the Langmuir isotherm. The micropore volume was estimated with the t-plot method.

UV-Vis diffuse reflectance spectra were recorded in a Cary 5000 (Agilent) spectrophotometer and a Praying Mantis setup (Harrick). The range studied was 200–800 nm at a 1 nm resolution and a 600 nm/min scan rate. The spectra were converted to Kubelka-Munk units.

Table 1. Composition of catalysts Cu-CHA.

Catalysts	Si/Al	Cu (wt. %)	Fe (wt. %)	Cu/Al
CHArw	3.5	--	3.3	--
CHAnat	3.5	--	2.8	
1.3/CHAnat	3.5	1.3	2.8	0.22
2.8/CHAnat	3.5	2.8	2.8	0.51
6.5/CHAnat	3.5	6.5	2.8	1.15
1.2/SSZ-13	12	1.2	--	0.15
2.1/SSZ-13	12	2.1	--	0.26
14/SSZ-13	12	14	--	1.81

Results and discussion

Effect of Cu loading in NH₃- SCR-NO

Fig. 1 shows the results for the NO conversion during reaction with CHAnat and SSZ-13 catalysts. Catalytic tests show that CHAnat without Cu has activity only at high temperature, i.e. a 30 % conversion of NO was obtained at 600 °C. This is probably caused by the presence of Fe species in the material [13]. In the case of SSZ-13 without Cu, the NO conversion was negligible in the full range of temperature studied.

With natural materials, there is the question of which is the zeolitic phase that is active for deNO_x. Our natural Chabazite contains about 16 % Clinoptilolite and 7 % Erionite. The literature has a report on the activity for SCR-NO with NH₃ of another natural zeolite containing 75 % clinoptilolite in which Fe was exchanged [14]. In the absence of Fe, the activity was low (20 % conversion at about 300 °C). With exchanged Fe the natural material had good activity in the region where our Cu/CHAnat catalyst was also active. Its activity was at the most similar to that of our material. In the case of Erionite, there is one report of a synthetic material exchanged with Cu as a deNO_x catalyst with NH₃ [15]. The activity results are difficult to compare with ours because the authors used much lower NO and NH₃ concentrations and space velocity in their study. The material was also unstable under high temperature treatments. To summarize this topic, it is possible that part of the deNO_x activity of our Cu-CHAnat material stems from the Clinoptilolite and Erionite phases, but we are confident to assert that their contribution does not surpass their fractional content.

The exchange of 1.3 wt. % Cu in CHAnat led to a maximum in NO conversion of 58 % at 300 °C and the conversion remained above 50 % until 600 °C. The ignition temperature was roughly 200 °C. In the case of SSZ-13, the addition of 1.2 wt.% Cu resulted in a 100 % NO conversion at 420-520 °C. A closer look at the conversion-temperature trace in this case shows that there are 3 different regimes, the first one between 150 and 200 °C where a NO conversion of 35 % is reached; the second regime extends from 220 to 300 °C (similar to the one observed with 1.3/CHAnat), where the conversion reaches 80 %; a third regime is seen between 340 and 500 °C, where NO conversion rises to 100 %. With both catalysts the conversion of NO decreases as the temperature is further increased. That is observed to occur around 400 °C for 1.3/CHAnat and 500 °C for 1.2/SSZ-13. The decrease in NO conversion appears to be caused by a shift in the NH₃ reaction selectivity as a result of its direct oxidation with O₂ to NO and NO₂.

The low activity of 1.3/CHAnat at temperatures above 300 °C, when compared with 1.2/SSZ-13 is probably caused by the presence of inert cations and metal oxides in the zeolite limiting exchange or blocking active sites for SCR-NO. The 1.2/SSZ-13 does not have those limitations.

An increase in the Cu content to the intermediate range caused an increase in the activity of both zeolites. That was evidenced by a 50 °C decrease in the ignition temperature and a 100 % NO conversion between 250-400 °C for the 2.8/CHAnat catalyst. With 2.1/SSZ-13, the NO conversion was 100 % between 240-450 °C, with a single ignition temperature.

When Cu increased to 6.5 wt.% in CHAnat, the maximum conversion decreased to 93 % between 250-400 °C. In the case of 14/SSZ-13, the NO conversion was 100 % between 230-400 °C. At higher temperatures, the NO conversion decreased rapidly probably because of the formation of Cu moieties that favor the oxidation

of NH_3 by O_2 under those conditions. The loss in activity for the CHAnat sample suggests either site blockage and/or the formation of dimers or proto-oxides of Cu in the zeolite. These Cu species may be located inside or outside the main zeolite framework depending on their size.

Our results point out to the existence of an optimal Cu loading in the chabazite zeolites, this being around 2 wt.%. This coincides with literature reports that place the optimum between 2 and 3.4 wt.% Cu [1,3,4]. It is important to mention that all our catalysts showed low production of N_2O (<5 ppm) in the temperature range studied.

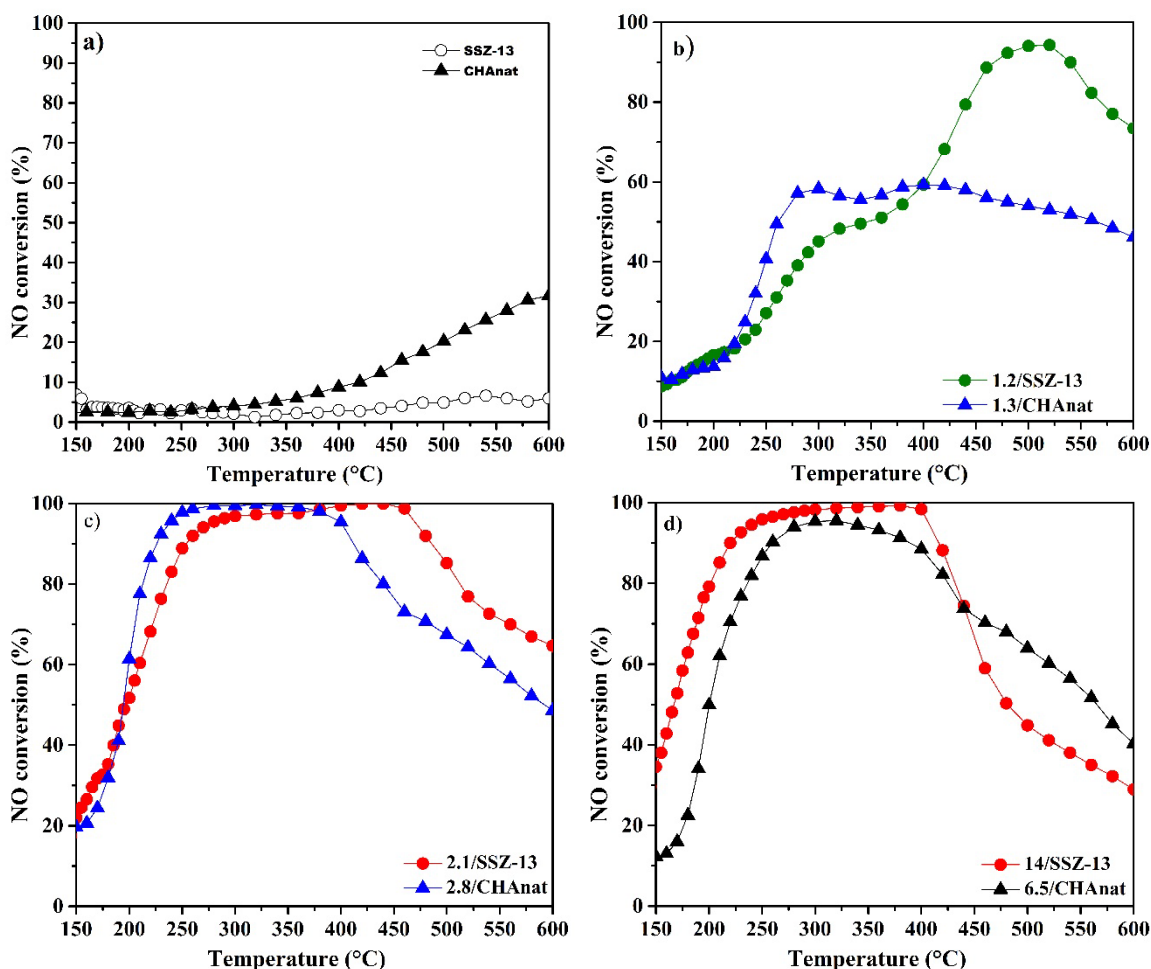


Fig. 1. NO conversion versus reaction temperature for standard NO-SCR. **a)** SSZ-13 and CHAnat, **b)** 1.2/SSZ-13 and 1.3/CHAnat, **c)** 2.1/SSZ-13 and 2.8/CHAnat & **d)** 14/SSZ-13 and 6.5/CHAnat. Reaction feed: 500 ppm NO, 500 ppm NH_3 , 2.5% O_2 , and balance N_2 .

Cu-based average rate of reaction

To further analyze the effect of Cu on the catalytic behavior of our samples, we estimated the average reaction rate per mole of Cu and present those results in Fig. 2.

For the low and medium Cu loading catalysts the trend is similar, the catalysts based on SSZ-13 have higher average rates throughout the whole temperature range than those synthesized with CHAnat. Fig. 2a) shows the results for 1.2/SSZ-13 and 1.3/CHAnat, and Fig. 2b) has the results for 2.1/SSZ-13 and 2.8/CHAnat.

Interestingly, the low loaded zeolites have higher average rates per Cu site than the medium loaded materials, suggesting that the Cu species are more readily accessible for NO-SCR when small amounts of active sites are present in the catalyst. The absolute value of the rate also has that trend as the Cu loading increases. It appears that a trade-off is reached with the medium-loaded catalysts, where accessibility and number of sites are balanced. At high Cu loading, the average rate per Cu site decreases significantly (Fig. 2c), and there is a flip between SSZ-13 and CHAnat-based catalysts. In this case, the amount of Cu present in SSZ-13 is twice as large as in CHAnat, leading to the presence of Cu species that are presumably inactive for SCR in SSZ-13. A note of caution is warranted, as in part of the temperature range some of the catalysts caused 100% conversion and the measurement of their actual activity was hence limited by the experimental conditions. We are analyzing the role of higher space velocities, but the results presented here are globally correct.

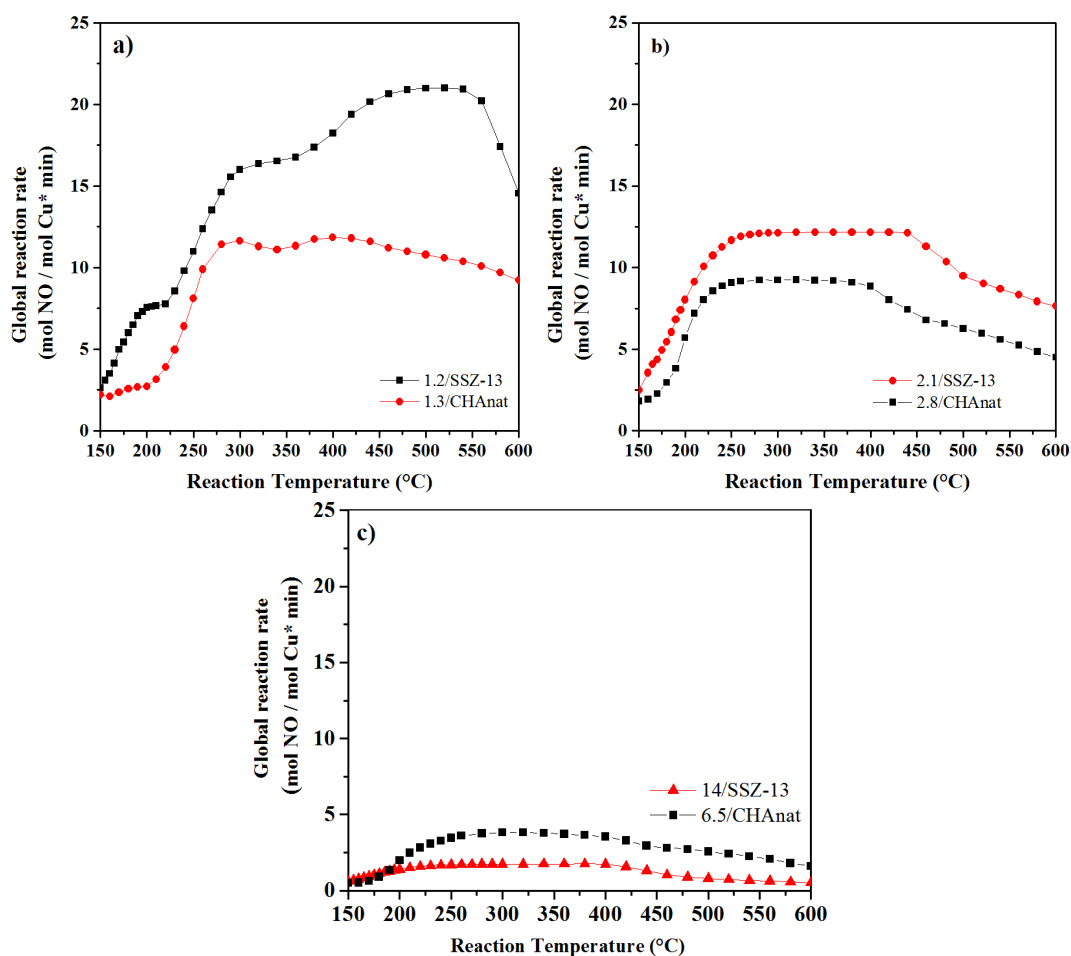


Fig. 2. Global reaction rate versus reaction temperature for standard SCR-NO with NH_3 . **a)** 1.2/SSZ-13 and 1.3/CHAnat, **b)** 2.1/SSZ-13 and 2.8/CHAnat & **c)** 14/SSZ-13 and 6.5/CHAnat. Reaction feed: 500 ppm NO, 500 ppm NH_3 , 2.5% O_2 , and balance N_2 .

Catalyst characterization

To determine a possible effect of the structure upon the reactivity of our catalysts, we analyzed them using X-ray diffraction, N_2 adsorption and UV-Visible diffuse reflectance spectroscopy.

X-ray diffraction

Fig. 3a) shows XRD patterns for SSZ-13 and Cu-exchanged SSZ-13. The characteristic reflections of Chabazite are present and the samples have high crystallinity, 89 % for CHAnat and 96 % for SSZ-13 [21]. Catalysts with 1.2 wt.% and 2.1 wt.% Cu do not present CuO peaks ($2\theta = 35.6^\circ$ and 38.8°), an indication that Cu species are either well dispersed or exist as ions at the exchange sites.

The intensity of the diffraction peak at 9.5° (diffraction from the (100) plane of the CHA structure) of 14/SSZ-13 is much lower than those of the other catalysts, indicating that more Cu^{2+} ions are located inside the CHA cages next to the 8-membered rings over 14/SSZ-13. It has been reported that Cu^{2+} ions cause the deformation of the 8-membered rings, which leads to a weakening of diffraction from the (100) plane of the CHA structure [21,22].

Fig. 3b) shows the XRD patterns for CHArAw,(as-received) and Cu/CHAnat catalysts, which includes diffraction lines at 9.4° , 12.8° , 20.4° , 30.4° , and 30.7° corresponding to (100), (-100), (-210), (-311) and (310) crystal planes characteristic of chabazite (JCPDS 52-0784). The powder X-ray diffractogram of CHArAw (as-received) also shows characteristic reflections of Clinoptilolite and Erionite with a good degree of crystallization. The crystallinity of Chabazite decreased after washing, from 89.8 to 84.8 %, as well as that of Clinoptilolite (85.0 to 57.01 %), whereas that of Erionite increased (40.5 to 43.3 %). Zeolites present in natural chabazite were quantified using the MAUD software. After washing and calcining the chabazite increased its percentage from 60 to 77 %, the clinoptilolite decreased from 32 to 16 % and the erionite remained at 7%. These changes, as well as those in crystallinity reflect the labile nature of the clinoptilolite during calcination. Fe species reflections were not observed probably because of their high dispersion or poor crystallinity. Catalysts with 1.3-6.5 wt. % of Cu did not show reflections for CuO, Cu_2O , or Cu, due to its low content (when is the case) or high dispersion. One must remember also that most Cu was presumably present as charge balance cations in the zeolites. The incorporation of Cu did not affect the structure of the CHA.

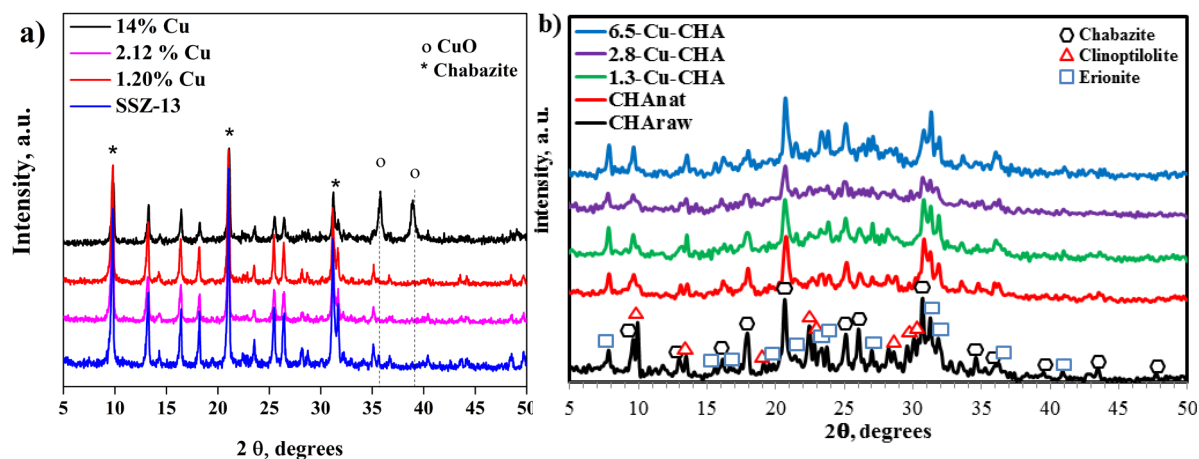


Fig. 3. XRD patterns for a) SSZ-13 and b) CHAnat with different copper loadings.

Textural properties

The N_2 adsorption-desorption isotherms of the calcined samples are given in Fig. 4. There were differences in the adsorption capacity between SSZ-13 and CHAnat.

SSZ-13 had a type IA isotherm, typical of microporous materials [16]. There was no hysteresis loop because of the homogeneous porosity of this type of material. For relative pressures $P/P_0 < 0.1$, the amount of adsorbed N_2 increases rapidly and levels off, it increases only slowly in the relative pressure range $0.1 < P/P_0 < 0.9$ as expected for a typical microporous structure. The surface area of SSZ-13 was $640 \text{ m}^2/\text{g}$ with a micropore and mesopore volume of $0.366 \text{ cm}^3/\text{g}$ and $0.020 \text{ cm}^3/\text{g}$, respectively.

The isotherm for CHANat was a type I and IV according to the IUPAC classification, which indicates the presence of both microporosity and mesoporosity. Steep uptake of the physisorption isotherm of CHANat at relative pressure of $P/P_0 < 0.1$ is caused by the micropore filling. There was a hysteresis loop at relative pressure of $P/P_0 > 0.3$, an indication of a secondary capillary condensation process taking place in the mesopores. The shape of the hysteresis loop in the CHANat is type H4.

The mesoporosity of CHANat may be caused by presence of different phases in the natural zeolite, some which may not be zeolitic, as well as by its production process, that involves grinding and milling of the mined material. CHANat has a surface area of $629 \text{ m}^2/\text{g}$, micropore volume of $0.184 \text{ cm}^3/\text{g}$ and mesopore volume of $0.165 \text{ cm}^3/\text{g}$. (Fig. 4). The micropore volume of SSZ-13 is definitively higher than that of CHANat ($0.366 \text{ cm}^3/\text{g}$ vs. $0.184 \text{ cm}^3/\text{g}$), while the mesopore volume of the CHANat is substantially higher ($0.164 \text{ cm}^3/\text{g}$ vs. $0.02 \text{ cm}^3/\text{g}$). Part of the difference between CHANat and SSZ-13 lies in their different purity and crystallinity.

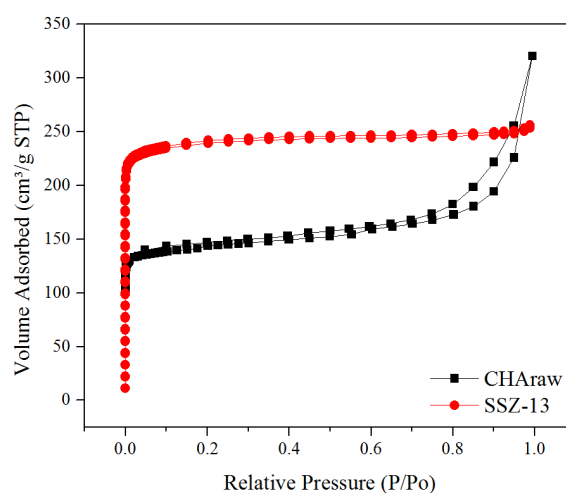


Fig. 4. N_2 adsorption isotherms of CHANat and SSZ-13 at 77 K.

Ultraviolet-visible diffuse reflectance spectroscopy

For the Cu/SSZ-13 catalysts the UV-Vis DR-spectra with different copper loadings before reaction (fresh) and after reaction are presented in figures 5a), 5c), and 5e). The 1.2/SSZ-13 fresh catalyst presents two absorption bands, one between 200-260 nm centered at $\sim 217 \text{ nm}$ assigned to the ligand to metal charge transfer ($\text{LMCT O}_{2\text{CHA}} \rightarrow \text{Cu}^{2+}$), and the other band in the spectral range 600-1200 nm (d-d transition for Cu^{2+}). Both bands increased in intensity as the Cu loading increased from 1.2 to 2.1 wt. % due to an increase in the population of Cu absorption sites [17]. This observation agrees with Negri et al. and Ipek et al. [17,18] and it is linked to a homogeneous distribution of -OH coordinated to Cu ions in their hydrated state. The first absorption band appears at 230 nm in the 2.1/SSZ-13 catalyst and shifts after reaction towards 250 nm (Cu^{2+} species). That signal and the band between 500-800 nm increase in intensity after the catalyst is used in the reaction, signaling a structural change presumably via a redistribution of the Cu^{2+} sites. After reaction, the spectra for the 14/SSZ-13 catalyst had, in addition to a similar signal shift at high energy, a new band with strong absorption between 300 and 870 nm, which suggests the appearance of Cu nanoparticles, as well as large size CuOx. This assignment agrees with our XRD results. These species have been reported to play a role in the non-selective oxidation of NH_3 at high temperatures [19–21].

The spectra of Cu/CHANat catalysts with different copper loadings before (fresh) and after reaction are presented in figures 5b), 5d), and 5f). The fresh 1.3/CHANat catalyst shows bands between 200-300 nm, which could correspond to the $\text{LMCT O}_{2\text{CHA}} \rightarrow \text{Cu}^{2+}$ observed in Cu/SSZ-13 catalysts; the bands between 300-600 nm correspond to O-Cu-O and Cu-O-Cu dimeric species and possibly Cu^0 nanoparticles and the band between 600-1200 nm has been assigned to d-d transition of Cu^{2+} [22–24]. When the loading of Cu increased

to 2.8 wt. % all bands increased in intensity also suggesting a change in the distribution of Cu species [17,18]. It corresponds to a homogeneous distribution of -OH coordinated to Cu ions in their hydrated state. The high energy band in the 200-600 nm region (Cu^{2+} and Cu dimers) of 2.8/CHANat increased in intensity after reaction, and so did the d-d band transition of Cu^{2+} between 500-800 nm. suggesting a possible redistribution of the Cu^{2+} species. When the loading of Cu was 6.5 wt.%, the band of Cu^{2+} was similar in intensity to that of 2.8/CHANat. While the bands of Cu-O-Cu and O-Cu-O dimeric species had low intensity and the d-d transition bands of Cu^{2+} increased further. The presence of copper oxide nanoparticles of large size was not observed in Cu/CHANat nor in Cu/SSZ-13 catalysts with low and intermediate Cu loading, because there was no band at 650 nm, a signature for those nanoparticles.

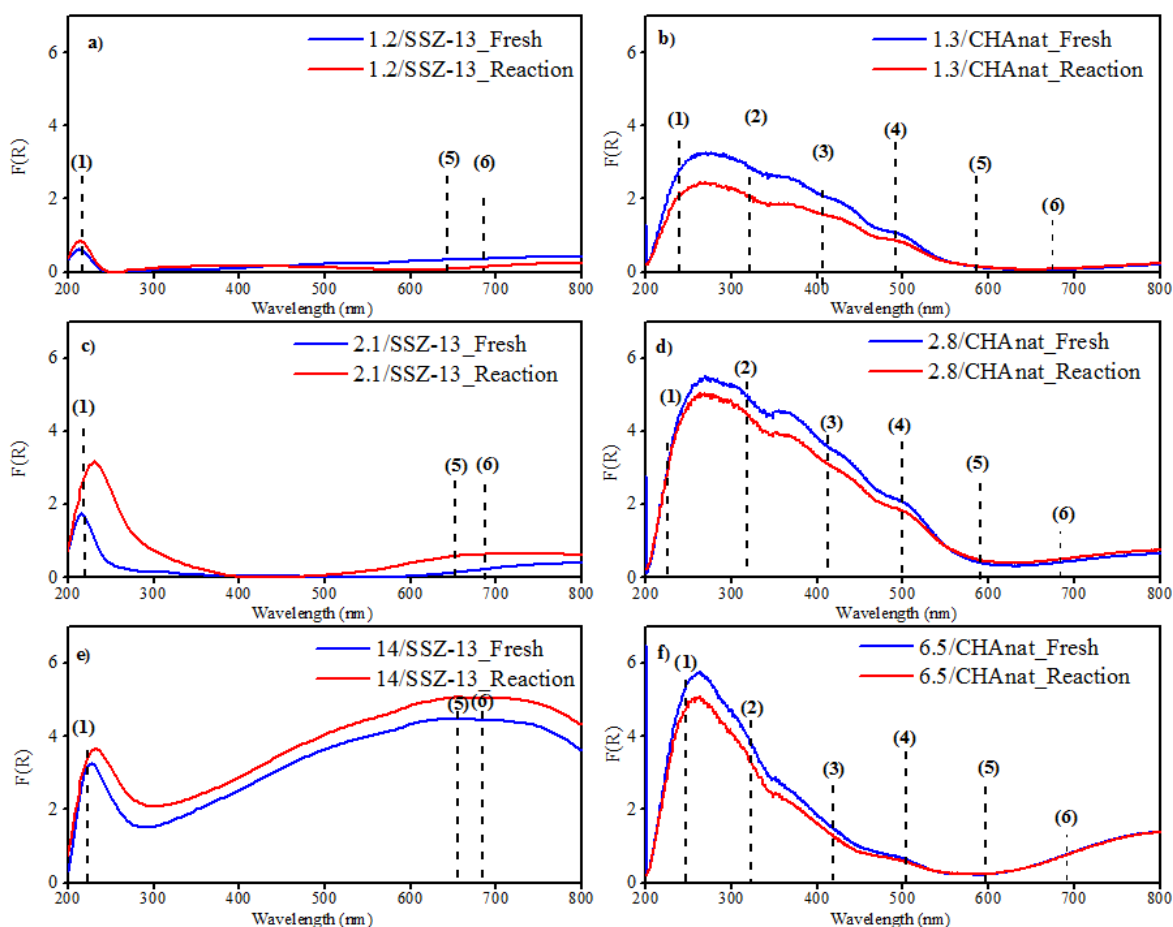


Fig. 5. UV-Vis DR-spectra for fresh and spent catalysts after NH_3 -SCR-NO reaction. Arrows correspond to bands associated with $\text{O} \rightarrow \text{Cu}^{2+}$ (1), O-Cu-O (2), Cu-O-Cu (3), Cu^0 nanoparticles (4), d-d transitions in Cu^{2+} (5) and CuO (Bulk) (6).

After using the chabazite catalysts in reaction there were changes in Cu^{2+} coordination and variation in the intensity of absorption. The bands of Cu/SSZ-13 catalysts increased in intensity while the bands of Cu/CHANat catalysts decreased, in both cases the variations in the absorption bands may be explained by the redox cycle undergone by Cu during the reaction of NO with NH_3 .

Catalysts 1.2/SSZ-13 and 1.3/CHANat only reached high conversion at high temperatures, what may be correlated with the small presence of Cu^{2+} signals. There was no evidence of dimeric species in the UV vis spectra. Catalysts 2.1/SSZ-13 and 2.8/CHANat presented high activity in NH_3 -RCS-NO in a wide temperature range that can be explained by the increased concentration of isolated Cu^{2+} ions and low population of Cu dimers. That is not the case of the catalysts with high Cu loading as 14/SSZ-13 and 6.5/CHA. These catalysts have high activity at lower temperatures (150-300 °C), but after 300 °C the activity decreases sharply, probably caused by the presence of bulk CuO evidenced by spectral bands in the 600-800 nm range.

Effect of Si/Al ratio in NO-SCR with NH_3

As reported in Table 1, there was a significant difference in the Si/Al ratio for the two zeolitic materials. It is well known that the Si/Al ratio plays an important role in zeolites because it determines the exchange capacity, Cu speciation, acidity, and thermal stability [21]. Those differences may result in variations in the Cu species exchanged in every zeolite. For example, it is reported that with a low Si/Al ratio and at low Cu loading, Cu^{2+} ions are expected to be close to the 6 MR windows and bind to 2 Al sites. Conversely, with high Si/Al ratio, the possibility of finding 2 Al sites in a 6 MR ring is unlikely. In that case, it is possible that Cu^{2+} ions interact with two distant Al sites (e.g. 2 Al sites in 8MR). According to other reports [21,22], there could be another alternative: Cu ions at high Si/Al ratio zeolites can balance only one Al site, but in this case Cu species like Cu^+ or Cu complexes like $[\text{Cu}^{2+}(\text{OH})]^+$ are required to balance the negative charge in the framework [21,23]. The UV-Vis spectra indicate that CHANat catalysts had different Cu species, not only Cu^{2+} as in the case of Cu/SSZ-13 catalysts. The same occurred at high Cu contents, where we have more than one type of Cu, which are not necessarily active for the NO-SCR reaction [21,24]. At close Cu contents (2.1 and 2.8 wt %), we observe that the catalytic activity was comparable, probably resulting from a similar population of Cu^{2+} sites.

Conclusions

We compared two zeolites with a similar structure but of a different nature (natural and synthetic). The textural analysis showed that natural chabazite has mesopores and micropores and the SSZ-13 only has micropores.

The Cu/CHA and Cu/SSZ-13 catalysts had high activity to reduce NO in the presence of NH_3 . At a low copper content of 1.2 wt. %, the activity was higher for the catalyst based on SSZ-13, reaching a NO conversion of 90 % at high temperatures (300-600°C), while natural chabazite only attained 50 %. The best results were obtained with copper loadings in the 2-3 wt.% range for both materials, attaining complete NO conversion in the temperature range adequate for SCR-NO. A high Cu loading allowed a good conversion of NO at low temperatures, 150-300 °C with SSZ-13, but that affected negatively the activity of the natural zeolite catalyst.

The catalytic activity was different because of variations in the population and distribution of Cu species present as evidenced by ex-situ DR-UV-Vis. Cu species were identified in the 2.8/CHA catalyst as Cu^{2+} , O-Cu-O, Cu-O-Cu, and the possible presence of Cu^0 nanoparticles. The 2.1/SSZ-13 material, on the other hand, had primarily Cu^{2+} species and low presence of CuOx moieties. The presence of Cu^{2+} ions in Cu/CHANat and in Cu/SSZ-13 suggests that these sites are responsible for the activity. After the reaction, there were changes in the intensity of the bands corresponding to Cu^{2+} in all the catalysts, suggesting their possible restructuring.

Acknowledgements

The authors acknowledge the support from project CB-166363 of CONACYT and UAM-Iztapalapa. We thank St. Cloud™ Mining Company for a sample of natural chabazite, Prof. Raul Lobo's Group at Univ. of Delaware for their help in the synthesis of zeolites and SACHEM Inc. for the SDA. Julio Lopez-Curiel, Gabriela Hernández-Salgado and María Eugenia Hernández-Terán thank CONACYT for their graduate fellowships.

References

1. Qi, G.; Yang, R. T.; Chang, R. *App. Catal., B* **2004**, 51, 93–106.
2. Si, Z.; Weng, D.; Wu, X.; Li, J.; Li, G. *J. Catal.* **2010**, 271, 43–51.
3. Sjövall, H.; Blint, R.J.; Olsson, L. *App. Catal., B* **2009**, 92, 138–153.
4. Kwak, J.H.; Tran, D.; Szanyi, J.; Peden, C.H.F.; Lee, J.H. *Catal. Lett.* **2012**, 142, 295–301.
5. Fickel, D.W.; D'Addio, E.; Lauterbach, J.A.; Lobo, R.F. *App. Catal., B* **2011**, 102, 441–448.
6. Stacey I. Zones, U S Patent **1985**, 4, 544, 538.
7. Komatsu, T.; Nunokawa, M.; Moon, I.S.; Takahara, T.; Namba, S.; Yashima, T. *J. Catal.* **1994**, 148, 427–437.
8. Kieger, S.; Delahay, G.; Coq, B. *App. Catal., B* **2000**, 25, 1–9.
9. Kefirov, R.; Penkova, A.; Hadjiivanov, K.; Dzwigaj, S.; Che, M. *Microporous Mesoporous Mater.* **2008**, 116, 180–187.
10. Bull, I.; Xue, W.M.; Burk, P.; Boorse, R.S.; Jaglowski, W.M.; Koermer, G.S.; Moini, A.; Patchett, J.A.; Dettling, J.C.; Caudle, M.T.; Llc, B.C. Patent **2008**, US 7,601,662 B2, BASF Catalysts LLC.
11. Kwak, J.H.; Tonkyn, R.G.; Kim, D.H.; Szanyi, J.; Peden, C.H.F. *J. Catal.* **2010**, 275, 187–190.
12. Pham, T.D.; Liu, Q.; Lobo, R.F. *Langmuir* **2013**, 29, 832–839.
13. Anunziata, O.A.; Beltramone, A.R.; Juric, Z.; Pierella, L.B.; Requejo, F.G. *App. Catal., A* **2004**, 264, 93–101.
14. Gelves, J.F.; Dorkis, L.; Márquez, M.A.; Álvarez, A.C.; González, L.M.; Villa, A.L. *Catal. Today* **2019**, 320, 112–122.
15. Martín, N.; Paris, C.; Vennestrøm, P.N.R.; Thøgersen, J.R.; Moliner, M.; Corma, A. *App. Catal., B* **2017**, 217, 125–136.
16. Thommes, T.; Kaneko, K.; Neimark, A.V.; Olivier, J.P.; Rodriguez-Reinoso, F.; Rouquerol, J.; Sing, K.S.W. *Pure App. Chem.* **2015**, 87, 1051–1069.
17. Negri, C.; Signorile, M.; Porcaro, N.G.; Borfecchia, E.; Berlier, G.; Janssens, T.V.W.; Bordiga, S. *App. Catal., A* **2019**, 578, 1–9.
18. Ipek, B.; Wulfers, M.J.; Kim, H.; Göltl, F.; Hermans, I.; Smith, J.P.; Booksh, K.S.; Brown, C.M.; Lobo, R.F.; *ACS Catal.* **2017**, 7, 4291–4303.
19. Gang, L.; van Grondelle, J.; Anderson, B.G.; van Santen, R.A. *J. Catal.* **1999**, 186, 100–109.
20. Pestryakov, A.N.; Petranovskii, V.P.; Kryazhov, A.; Ozhereliev, O.; Pfänder, N.; Knop-Gericke, A. *Chem. Phys. Lett.* **2004**, 385, 173–176.
21. Gao, F.; Walter, E.D.; Washton, N.M.; Szanyi, J.; Peden, C.H.F. *App. Catal., B* **2015**, 162, 501–514.
22. Wang, L.; Gaudet, J.R.; Li, W.; Weng, D. *J. Catal.* **2013**, 306, 68–77.
23. Giordanino, F.; Vennestrøm, P.N.R.; Lundegaard, L.F.; Stappen, F.N.; Mossin, S.; Beato, P.; Bordiga, S.; Lamberti, C. *Dalton Trans.* **2013**, 42, 12741–12761.
24. Wang, D.; Zhang, L.; Li, J.; Kamasamudram, K.; Epling, W.S. *Catal. Today* **2014**, 231, 64–74.